IOSR Journal Of Applied Physics (IOSR-JAP)
e-ISSN: 2278-4861.Volume 15, Issue 1 Ser. I (Jan. – Feb. 2023), PP 28-33
www.Iosrjournals.Org

Fabrication of Ni_2O_3: Al Thin Films as Alternative for Transparent Electrodes Using Advanced Successive Ionic Layer Adsorption and Reaction (ASILAR) Method

Joseph Ijeoma Onwuemeka[1] Ph.D. and Margaret Chinyelu Enedoh[2] Ph.D.
Corresponding Author: Joseph Ijeoma Onwuemeka[1], Email:josephijeoma@yahoo.com

ABSTRACT
Nickel oxide thin films doped with aluminum have been fabricated using advanced SILAR deposition technique on glass substrates. These films have been characterized using Rutherford backscattering for elemental composition and thickness measurements, UV double beam spectrophotometer 1800 series for optical measurements. Ni_2O_3:Al thin films have high transmission in the wave length range of 300–1100 nm. The film samples A_1 and A_2 have average band gap of 3.25eV ± 0.05eV

Date of Submission: 10-01-2023 Date of Acceptance: 26-01-2023

I. INTRODUCTION

Nickel(II) oxide is the chemical compound with the formula NiO. It is the principal oxide of nickel. Nickel oxide (NiO) is an important material mostly used for catalysis, battery cathodes (Yoshio, 1998), gas sensors, electro-chromic films (Alcantara, 1998; Wu, 2007). The nickel oxide thin films were deposited using numerous methods i.e. thermal evaporation (Patel 2011), organic solvent method (Velevska, 2011) chemical vapor deposition, electro-chemical deposition, sol–gel (Nalage, 2012) chemical solution deposition (Vidales-Hurtado, 2008). Among all these deposition techniques, SILAR is preferable due its inexpensive, low-temperature synthesis and the possibility of depositing materials on various substrates. Recently, semi-transparent p-type conducting films of the nickel oxide (NiO) have attracted considerable attention because of their importance in several scientific applications, in the areas of : material for electrochromic display devices (Sun *et al*, 2018; Kitao *et al*, 1994), as functional sensor layers in chemical sensors (Kumagai *et al*,1996) and transparent electronic devices (Zhang *et al*, 2018) and the magnetic properties of nanoparticles (Tiwari & Rajeev, 2016; Arif *et al*, 2019). NiO thin film is an insulator at room temperature (resistivity is ~10^{13} Ω·cm) (Adler & Feinleib, 1970). Much effort has been made to explain the insulating behaviour of NiO. It has an optical band gap range of 3.4-4.0 eV (Ai *et al*, 2008). In this work, the influence of Al doping on Ni_2O_3 thin films will be studied using advanced SILAR method and its effects on elemental compositions, thicknesses and optical properties.

II. MATERIALS AND METHOD

The synthesis of Ni_2O_3 thin films doped with Al^{3+} by advanced SILAR method constituted: 4ml of 3M solution of ammonia used as complexing agent, 10.45g of 1M solution of $NiCl_2{:}6H_2O$ dissolved in $100cm^3$ of water and H_2O_2 solution . 4ml of 3M solution of ammonia was made to react with 1M solution of $NiCl_2{:}6H_2O$ forming nickel tetra-amine complex ion as given in equations (1).

De-ionized water was added up to 50ml and the solution was stirred vigorously in order to achieve uniformity in the mixture. Ni_2O_3:Al thin films were deposited on substrates in cycles, by dipping the substrates into the beaker containing the cation precursor of nickel tetra-amine complex ions for adsorption of nickel ions and were rinsed in the second beaker of de-ionize water, then immersed into the third beaker, containing H_2O_2 solution as anion precursor, for adsorption of oxygen ions, the substrates were rinsed in the fourth beaker containing de-ionized water. The fifth beaker contains aluminum complex ion in which substrates containing the suspected nickel oxide were immersed and were rinsed in the sixth beaker containing de-ionized water. After successive immersions, the reactions on the various substrates are based on the varying number of cycles, while other parameters such as dip time, temperature (20^0C) volume and pH (5.6), were constant throughout the deposition processes. The reactions leading to the formation of nickel oxide doped aluminum are given in equations (1), (2) and (3). The deposition parameters for advanced SILAR deposition are given in Table 1 and the deposition processes are given in Figure 1.

$$2NiCl_2 : 6H_2O + NH_3 \longrightarrow 2[Ni(NH_3)_4]^{2+} + 4Cl^- + 12H_2O \quad (1)$$

$$2[Ni(NH_3)_4]^{2+} + 3H_2O_2 \longrightarrow Ni_2O_3 + 3H_2O + 8NH_3 \quad (2)$$

$$[Al(NH_3)_4]^{3+} + Ni_2O_3 \longrightarrow Ni_2AlO_3 + 4NH_3 \quad (3)$$

Table 1 The deposition parameters of Ni_2O_3 thin films.

Sample	Dip-time(s) in each reactant	No. of cycle	Dip-time(s) in each Beaker of H_2O
A_1	6	15	3
A_2	6	10	3
A_3	6	20	3
A_4	6	25	3
A_5	6	30	3

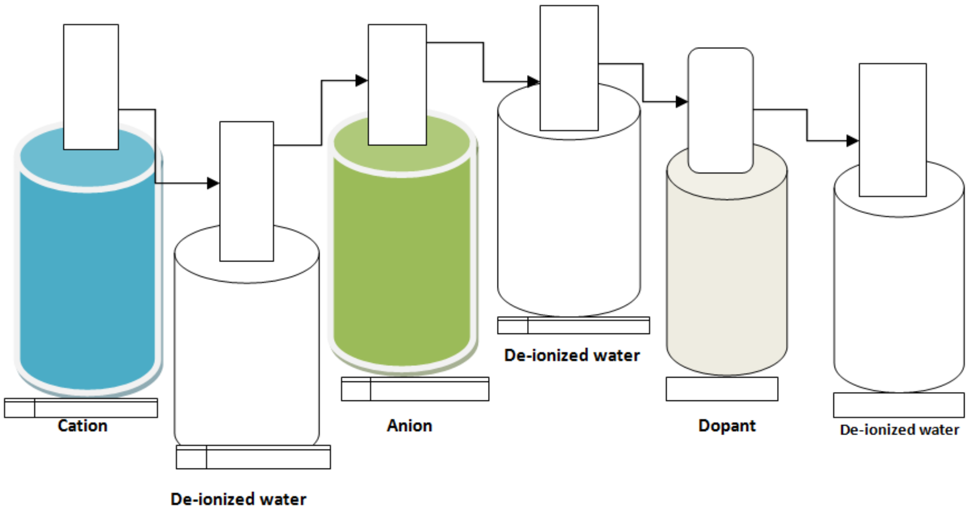

Figure 1 The Setup of Advanced SILAR Deposition Process

III. RESULTS AND DISCUSSIONS

In this work, atomic compositions and thicknesses were determined, using Rutherford backscattering Spectrometer (RBS) and the optical properties of the samples were measured using UV double beam spectrophotometer 1800 series.

THICKNESS MEASUREMENTS AND ELEMENTAL COMPOSITIONS

The Rutherford backscattering analysis shows that the samples A_1 with 10 cycles has thickness of 150nm and sample A_2 with 15 cycles has thickness 350nm as shown in Figures 2 and 3.

The elemental compositions of the two samples A_1: 90.50% of oxygen, aluminum 8.91%, nickel 0.49% and A_2: 85.10% of oxygen, aluminum 13.21%, nickel 1.54% . The entire samples were annealed at constant temperature of 250^oC. Also RBS results show that the longer the number of cycles, the thicker the sample materials, more cations will be deposited as well as the dopant.

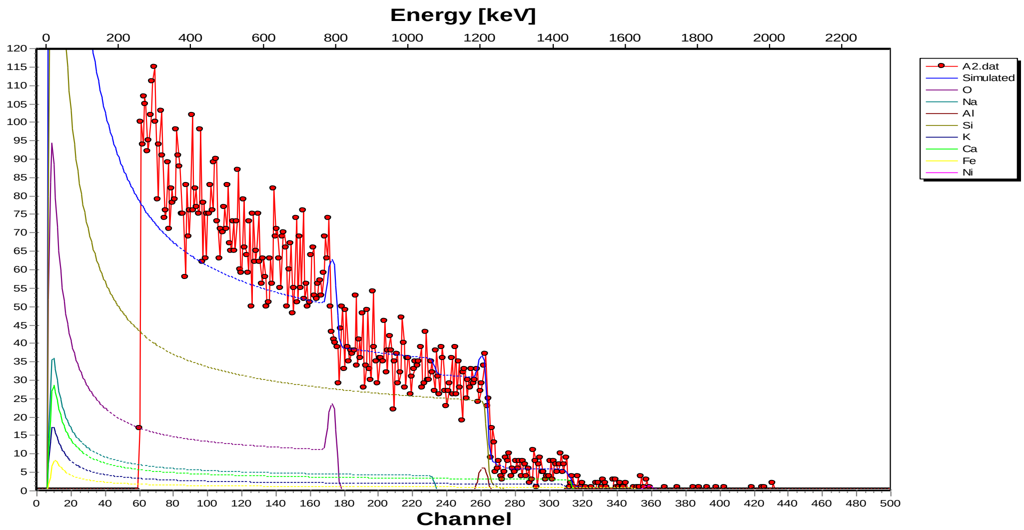

Figure 2 Elemental Composition of Sample A_1

LAYER 1: THICKNESS 150 nm
Compo: Ni 0.49% Al 8.91 % O 90.50%
LAYER 2: THICKNESS 5000 .0 nm
Compo: Si 35.19% O 51.02% Na 9.81% Ca 2.16% Al 0.02% K 1.41% Fe 0.39%

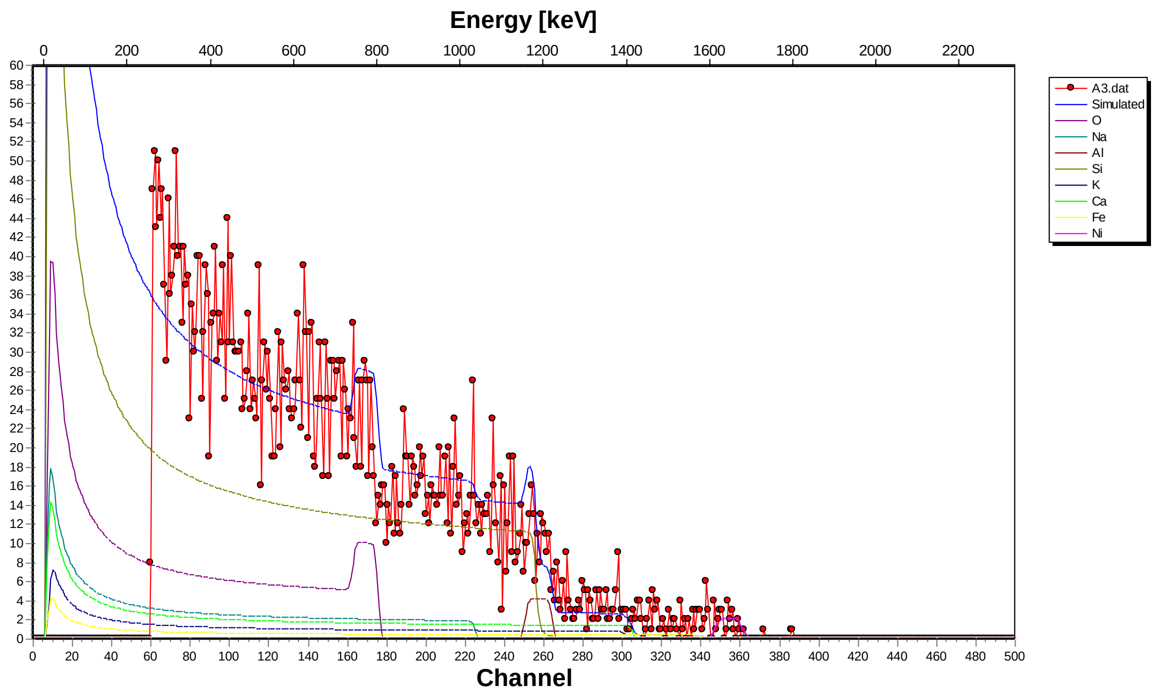

Figure 3 Elemental Composition of Sample A_2

LAYER 1: THICKNESS 350.0 nm
Compo: Ni 1.54% Al 13.21 % O 85.10%
LAYER 2: THICKNESS 5000.0 nm
Compo: Si 35.19% O 51.02% Na 9.81% Ca 2.16% Al 0.02% K 1.41% Fe 0.39%

Table 2 Transmittance of Sample A_1 and A_2

Wave length	Sample A_1	Sample A_2
300	0.4868	0.4939
350	0.7204	0.74988
400	0.77536	0.82593
450	0.77808	0.3818
500	0.78815	0.85464
550	0.79108	0.86325
600	0.79518	0.87117
650	0.7986	0.87599
700	0.79953	0.87976
750	0.79921	0.88084
800	0.80029	0.8828
850	0.80261	0.88608
900	0.80548	0.88963
950	0.80829	0.89275
1000	0.80998	0.89445
1100	0.81427	0.89752

Transmittance

The optical transmission data in the wavelength range 300nm to 1100nm in Table 2 were measured using UV double beam Spectrophotometer with serial number 1800. The range of transmittance was from 0.1 to 0.9 as the wavelength increases. Samples A_1 and A_2 share similar characteristics as depicts in Figure 4. The samples show high transmittance and can be used as cold and heat windows in infrared optics, transparent electrodes for optoelectronics and photonic applications since it has high transmittance in both visible and near infrared regions of electromagnetic spectrum.

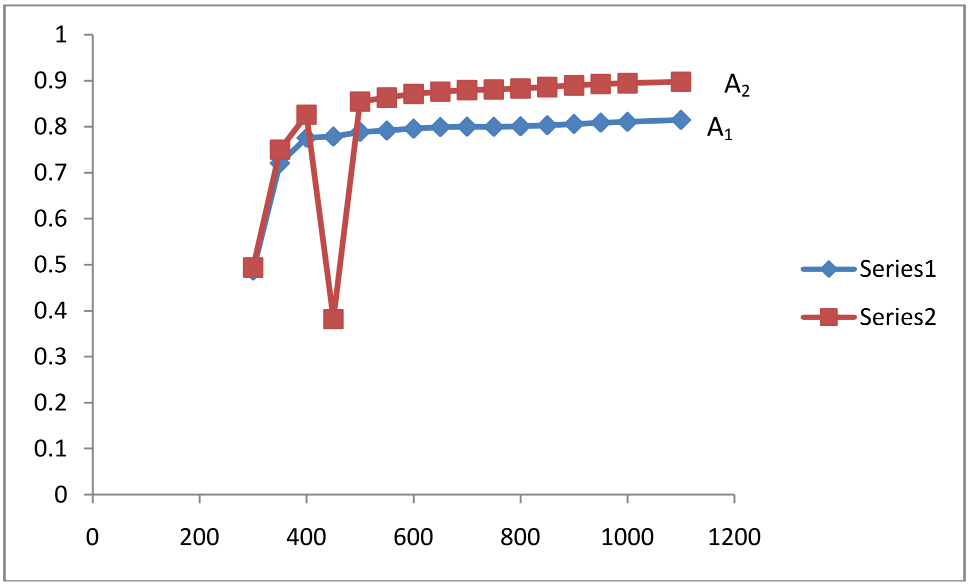

Figure 4 graph of transmittance against wavelength.

Absorbance

The absorbance shows a sharp decrease with increasing wavelength which indicates a shift from region of more absorbance to a region of less absorbance. Samples A_1 and A_2 share similar characteristics with low absorbance of the range 0.05 to 0.45. Both samples can be used as UV sensor and in UV spectroscopy. The graph of absorbance for the samples are shown Figure 5.

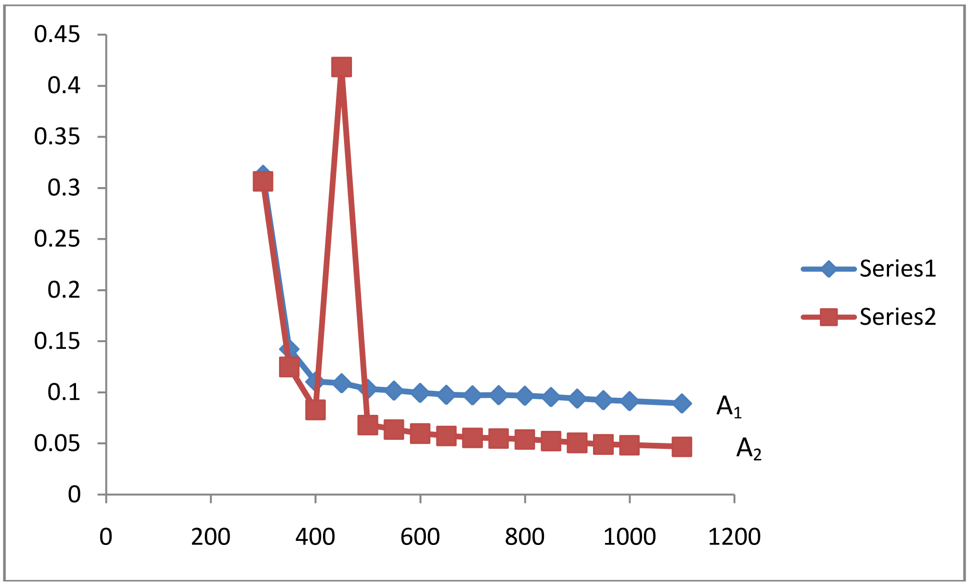

Figure 5 graph of absorbance against wavelength

Reflectance

This is the ratio of the reflected intensity to the incident intensity. The reflectance of the samples increased from 0.05 to 0.21. The samples have low reflectance, and can be used in multi-film technology to form anti-reflection coatings of almost zero reflectance in the visible region and for solar energy collectors. The graph of reflectance, R for the samples is shown in Figure 6.

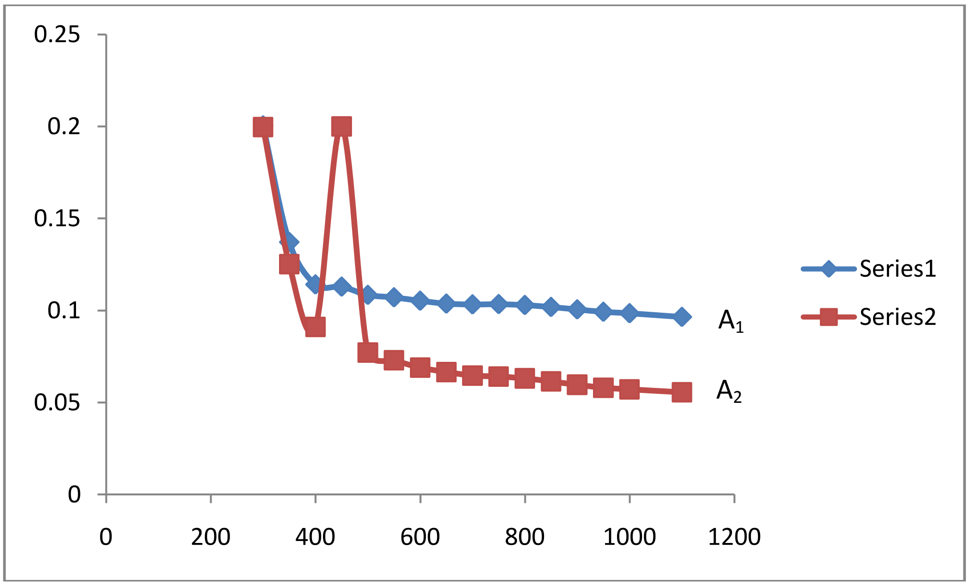

Figure 6 graph of reflectance against wavelength.

Table 3 Photon Energy and the squares of absorption coefficients of samples A_1 and A_2

Photon Energy (hv)	A_1 (α_1^^{2})	A_2(α_2^^{2})
4.144	2.30337E+13	4.06221E+12
3.552	4.78001E+12	6.76352E+11
3.108	2.87705E+12	2.98569E+11
2.763	2.79839E+12	7.56813E+12
2.487	2.51893E+12	2.01408E+11
2.26	2.44101E+12	1.76522E+11
2.072	2.33451E+12	1.55277E+11
1.913	2.2479E+12	1.43101E+11
1.776	2.2247E+12	1.33969E+11
1.658	2.23266E+12	1.31415E+11
1.554	2.20584E+12	1.26851E+11

1.463	2.14889E+12	1.19416E+11
1.381	2.07969E+12	1.11651E+11
1.309	2.01327E+12	1.05066E+11
1.243	1.97394E+12	1.01572E+11
1.13	1.87623E+12	95427814816

Energy band gap (E_g)

The band gap is determined from the graph of $(\alpha h\nu)^2$ against hv, by extrapolating the straight portion of the curve where αhv = 0 as given in Figure 7 as Table 3 gives the data parameters. A_1 and A_2 have average energy band gap of 3.25eV ± 0.05eV. This material can be found useful in the area of flat panel displays, FPDs, liquid crystal displays, LCDs, for electronic device applications.

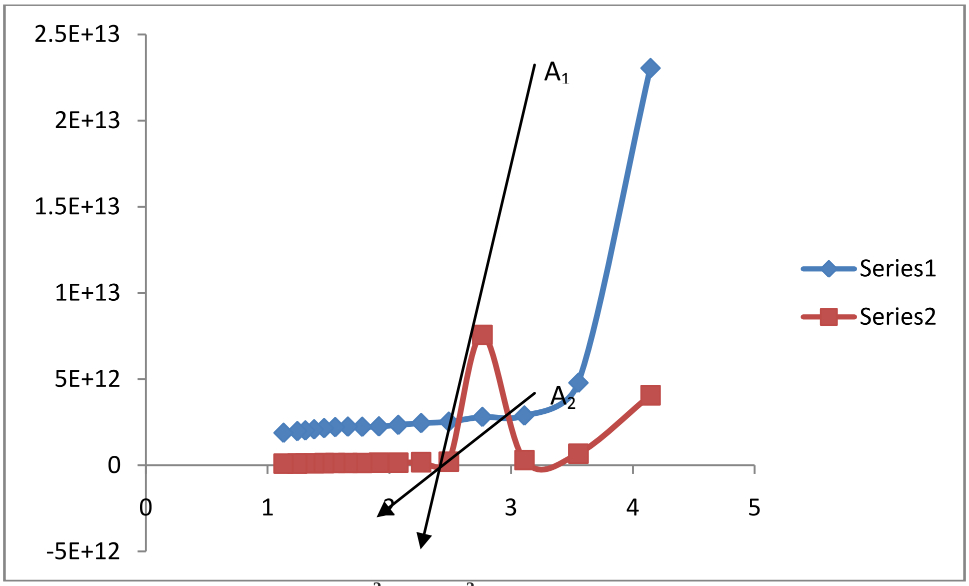

Figure 7 graph of $(\alpha h\nu)^2$ $(eV/m)^2$ against hv(eV) samples A_1 and A_2

IV. CONCLUSION

Synthesis of nickel oxide films doped with Al using advanced SILAR deposition technique have been reported. The average band gap of the films is 3.25 ± 0.05eV. The film sample A_2 prepared at 10 cycles has high transmission of 91% and the thin sample A_1 deposited at 15 cycles has transmittance of 83% which shows that the higher the number of cycles, the less the transmittance.

REFERENCE

[1]. Sun, H., Chen, S.C., Peng, W.C., Wen, C.K., Wang, X. & Chuang, T.H. The Influence of Oxygen Flow Ratio on the Optoelectronic Properties of p-Type Ni1−xO Films Deposited by Ion Beam Assisted Sputter. Coatings 2018, 8, 168.

[2]. Kitao, M., Izawa, K., Urabe, K., Komatsu, T., Kuwano, S. & Yamada, S. Preparation and electrochromic properties of rf-sputtered NiOx films prepared in Ar/O2/H2 atmosphere. Jpn. J. Appl. Phys. 1994, 33, 6656–6662.

[3]. Kumagai, H., Matsumoto, M., Toyoda, K. & Obara, M. Preparation and characteristics of nickel oxide thin film by controlled growth with sequential surface chemical reactions. J. Mater. Sci. Lett. 1996, 15, 1081–1083.

[4]. Tiwari, S.D. & Rajeev, K.P. Magnetic properties of NiO nanoparticles. Thin Solid Film. 2006, 505, 113–117.

[5]. Arif, M., Sanger, A., Shkir, M., Singh, A. & Katiyar, R.S. Influence of interparticle interaction on the structural, optical and magnetic properties of NiO nanoparticles. Phys. B 2019, 552, 88–95.

[6]. Adler, D. & Feinleib, J. Electrical and optical properties of narrow-band materials. Phys. Rev. 1970, B2, 3112.Nano-materials 2020, 10, 636 14 of 15.

[7]. Ai, L., Fang, G. Yuan, L., Liu, N., Wang, M., Li, C., Zhang, Q., Li, J. & Zhao, X. Influence of substrate temperature on electrical and optical properties of p-type semitransparent conductive nickel oxide thin films deposited by radio frequency sputtering. Appl. Surf. Sci. 2008, 254, 2401–2405.

[8]. Alcantara R, Lavela P, Tirado JL, Stoyanova R, Zhecheva E (1998), "Recent advances in the study of layered lithium transition metal oxides and their application as intercalation electrodes," J. Solid. State. Electrochem., 3(3): 121-134.

[9]. Nalage R S, Chougule A M, Sen S , Joshi B P, Patil B V (2012), "Sol–gel synthesis of nickel oxide thin films and their characterization," Thin Solid Films, 520 :4835–4840.

[10]. Patel J K, Desai S M, Panchal J C, Rehan B. "P-type transparent NiO thin films by e-beam evaporation techniques," J. Nano-Electron. Phys.,3 (1): 376-382, (2011)

[11]. Velevska J, Pecovska-Gjorgjevich M, Najdoski M and Stojanov N., (2011), "Studies on Electrochromism of Chemically Deposited Nickel Oxide Thin Films," Silpakorn U Science & Tech J., 5 (1): 34-42.

[12]. Vidales-Hurtado, A. M., Mendoza-Galván, A., (2008), "Electrochromism in nickel oxide-based thin films obtained by chemical-bath deposition," Solid State Ionics, 179: 2065–2068.